*Int. J. Electrochem. Sci.*, 14 **(2019)** 10448 – 10457, doi: 10.20964/2019.11.34

International Journal of
ELECTROCHEMICAL
SCIENCE
www.electrochemsci.org

*Short Communication*

# The Effect of Melt spun Treatment on the Properties of $La_4MgNi_{17}Co_2$ Hydrogen Storage Alloys

*Fansong Wei*[*], *Jianing Xiao, Hao Song*

School of Materials Science and Engineering, Jiangsu University of Science and Technology, Zhenjiang, Jiangsu Province, 212003, China
[*]E-mail: zjuwei@just.edu.cn

*Received:* 30 June 2019 / *Accepted:* 24 August 2019 / *Published:* 7 October 2019

The $La_4MgNi_{17}Co_2$ hydrogen storage alloys were prepared by induction melting, and the effect of melt spun treatment on the phase structure and electrochemical properties of the alloys were systematically investigated. The XRD analysis showed that all the alloys consist of $(La,Mg)_5Ni_{19}$ phase and $LaNi_5$ phase. Higher rapid solidification rate is beneficial to the formation of $A_5B_{19}$ phase. The electrochemical measurements showed that all the alloys have good activation performance (in 2 cycles) and high rate discharge-ability ($HRD_{600}$>87%). Higher rapid solidification rate can also improve the maximum discharge capacity ($C_{max}$) and capacity retention rate ($S_{100}$), such as the 25m/s alloy, $S_{100}$ = 71.27%, $C_{max}$ = 345.25 mAh/g. It is found that the $C_{max}$ variation of alloy electrodes are related with the phase abundance and cell volumes (*V*) of the two phases, and the improvement of cycling stability is due to the increasing of anti-pulverization of the alloys treated by melt spun method.

**Keywords:** hydrogen storage alloy; $A_5B_{19}$-type; crystal structure; electrochemical property; La-Mg-Ni system

## 1. INTRODUCTION

With the increasing demand for new energy, Nickel/metal hydride (Ni/MH) batteries have been widely studied and used, because they have many advantages, such as high capacity, good over charge/discharge resistance, excellent high rate discharge-ability and interchangeability with Ni-Cd batteries [1]. Among them, Ni/MH batteries with misch-metal-based $AB_5$-type alloys as anode material have been commercialized on a large scale. However, due to the limitation of $CaCu_5$-type structure, the intrinsic hydrogen storage capacity is not high for $AB_5$-type alloy, and the corresponding electrochemical discharge capacity is about 330 mAh/g, which limits its application [2].

In order to meet the demand of high energy density, the La-Mg-Ni system hydrogen storage alloys have been developed in all over the world. Among them, $AB_{3\sim3.8}$ series hydrogen storage alloys

have attracted wide attention due to their good hydrogen storage capacities. Kohno [3] et al found that the maximum discharge capacity of $La_{0.7}Mg_{0.3}Ni_{2.8}Co_{0.5}$ alloy can reach to 410 mAh/g, which is about 25% higher than that of $AB_5$-type alloys, but the cyclic life is poor (only 30 cycles). Nowadays there are several effective ways to improve the cyclic stability of hydrogen storage alloys, such as partial element substitution [4-13], non-stoichiometry [14-17], and preparation methods [18-25]. Liao [7,26] and Liu [12-14] studied the multi-element alloying of $La_2MgNi_9$ alloy by using Co, Al, Mn, Cu and Fe elements, and the results showed that the cyclic stability of La-Mg-Ni $AB_{3-3.5}$ alloy can be improved, and the capacity retention rate $S_{100}$ after 100 charge/discharge cycles is above 70%. Zhang et al [21-23] found that the melt spinning or annealing treatment can raise electrochemical cycle stability of the La-Mg-Ni system alloys, and the main reason was that these preparation methods enhanced the anti-pulverization ability of the alloys. Lv et al [24] reported that the $S_{100}$ of $La_{0.65}Ce_{0.1}Mg_{0.25}Ni_3Co_{0.5}$ alloy (30m/s) increases from 61.19% (as-cast) to 87.09%, but the maximum discharge capacity decreased obviously, and be lower than 250mAh/g. It is reported [27] that $A_5B_{19}$ phase has more anti-corrosion rate than the other phases in the La-Mg-Ni system hydrogen storage alloys. However, Mg element is easily volatile during melting, and studies [28-30] revealed that the $A_5B_{19}$ phase is difficult to be retained by conventional preparation for its easy decomposition. Previous work [6, 25] showed that the loss of Mg during melting can be reduced to 8% by using inter-alloys (Mg-Ni, or La-Ni), which can help to control accurate stoichiometric ratio and then retain more $A_5B_{19}$ phase. Thus, the $A_5B_{19}$-type $La_4MgNi_{17}Co_2$ hydrogen storage alloys were prepared by using inter-alloys and then melt spun at different solidification rates. The effects of rapid solidification rate on the crystal structure and electrochemical performances were discussed detailedly.

## 2. EXPERIMENTAL

The alloy samples were prepared by induction melting under argon atmosphere and then separately sprayed to the surface of a water-cooled rotating copper roller. The rapid solidification rate was expressed by the linear velocity of the copper roller with 10, 15, 20, 25m/s. The purity of all starting elemental metals is higher than 99.9%.

Such prepared alloy samples were crushed mechanically into powder below 50μm for electrochemical tests and X-ray diffraction (XRD) analysis. The phase identifications were carried out on a Rigaku D/max 2500/PC diffractometer with Cu $K_\alpha$ radiation by a step of 0.02º, and the range of 2θ data was from 20 º to 75º.

Alloy electrodes were prepared by cold pressing the mixtures of the alloy powder with carbonyl Ni powder in a mass ratio of 1:4 to form a pellet ($d$=10mm), and then tested at 298K in an open tri-electrode cell by using an automatic charge/discharge unit (Land) to obtain the electrical properties. The tri-electrode cell consists of a working electrode (MH electrode), a sintered Ni(OH) /NiOOH counter electrode and a Hg/HgO reference electrode, and the electrolyte was 6M KOH solution. Each electrode was galvanostatically charged at 120 mA/g for 4 h, and discharged at 60mA/g after 5min rest for activation. The cyclic stability was measured at the charge/discharge current of 300mA/g, and characterized by $S_{100}$ (capacity retention rate) = $C_{100}/C_{max}\times 100\%$, where $C_{100}$ was the discharge

capacities at 100$^{th}$ cycles, $C_{max}$ is the maximum discharge capacity. The high rate discharge-ability (HRD) was defined as $HRD_d = C_d / (C_d + C_{60}) \times 100\%$, where $C_d$ was the discharge capacity at different discharge current density (d=300, 600, 900 mA/g), $C_{60}$ is the residual capacity at 60 mA/g after $C_d$ was measured. The cut-off potential of all the tests above was -0.7 V (vs. Hg/HgO).

In order to further investigate the electrochemical kinetic properties of the electrodes, the linear polarizations were plotted by scanning the electrode potential at the rate of 0.1 mV/s from –5 to +5 mV (versus open circuit potential) at 50% depth of discharge (DOD), and the hydrogen diffusion coefficients were evaluated by the potentialstatic discharge technique, i.e. the test electrodes were discharged with +600mV potential-step for 3000 s after being fully charged and followed by a 30 min rest. All tests above were performed on a Sloartron SI1287 potentiostat, and then the results were analyzed by using the CorrWare software.

## 3. RESULTS AND DISCUSSION

### *3.1 Phase structure*

Fig. 1 shows the XRD patterns of as cast and melt spun $La_4MgNi_{17}Co_2$ alloys. It can be seen that all the alloys are composed of $(La,Mg)_5Ni_{19}$ phase ($Ce_5Co_{19}$+$Pr_5Co_{19}$, space groups are R-3m and $P6_3/mmc$ respectively) and $LaNi_5$ phase ($CaCu_5$ structure, space group: P6/mmm). With the increasing of rapid solidification rate, diffraction peaks of the melt spun alloys become wider. This result indicates that the grain size of the alloys is refined, and the internal stress or lattice distortion increases.

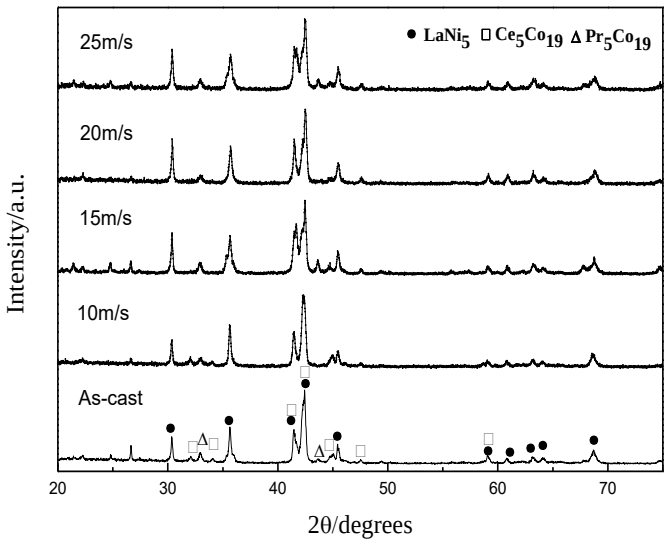


**Figure 1.** XRD patterns of as-cast and melt-spun $La_4MgNi_{17}Co_2$ alloys

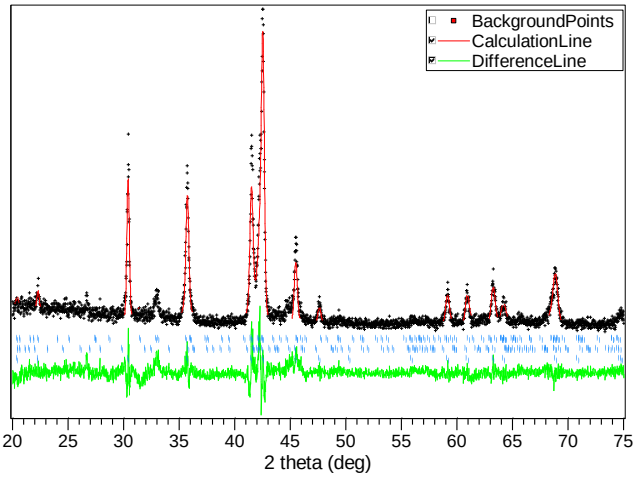


**Figure 2.** Calculate（line）and observed (+) X-ray diffraction patterns of $La_4MgNi_{17}Co_2$ alloy (20m/s)

Fig. 2 shows the XRD Rietveld analysis patterns of $La_4MgNi_{17}Co_2$ alloy (20m/s), in which the fitting factor ($R_p$) and reliability of fit ($S$) are 17.9 and 2.1 respectively. The Rietveld fitting results indicate that the Mg occupies the 4f and 6c positions in $A_5B_{19}$-type structure, which is same as Mg in $PuNi_3$ structure.

**Table 1.** The phase composition and Lattice parameters of as cast and melt spun $La_4MgNi_{17}Co_2$ alloys

| Samples | Phase | Space group | Phase abundance (*wt* %) | Lattice constants /nm | | Cell volume $V$ /$\times10^{-3}$nm$^3$ |
|---|---|---|---|---|---|---|
| | | | | *a* | *c* | |
| as cast | $LaNi_5$ | P6 /mmm (191) | 48.9 | 5.0299 | 3.9857 | 87.328 |
| | $Ce_5Co_{19}$ | R-3m (166) | 32.9 | 5.0426 | 48.4748 | 1067.490 |
| | $Pr_5Co_{19}$ | P63 /mmc (194) | 18.2 | 5.0481 | 32.1315 | 709.113 |
| 10 m/s | $LaNi_5$ | P6 /mmm (191) | 53.6 | 5.0298 | 3.9851 | 87.312 |
| | $Ce_5Co_{19}$ | R-3m (166) | 36.2 | 5.0437 | 48.4742 | 1067.922 |
| | $Pr_5Co_{19}$ | P63 /mmc (194) | 10.2 | 5.0488 | 32.1333 | 709.3505 |
| 15m/s | $LaNi_5$ | P6 /mmm (191) | 58.7 | 5.0256 | 3.9840 | 87.143 |
| | $Ce_5Co_{19}$ | R-3m (166) | 24.4 | 5.0439 | 48.4746 | 1068.016 |
| | $Pr_5Co_{19}$ | P63 /mmc (194) | 16.9 | 5.0462 | 32.1736 | 709.511 |
| 20 m/s | $LaNi_5$ | P6 /mmm (191) | 51.8 | 5.0250 | 3.9896 | 87.206 |
| | $Ce_5Co_{19}$ | R-3m (166) | 39.0 | 5.0494 | 48.5479 | 1071.984 |
| | $Pr_5Co_{19}$ | P63 /mmc (194) | 9.2 | 5.0478 | 32.2177 | 710.934 |
| 25 m/s | $LaNi_5$ | P6 /mmm (191) | 45.6 | 5.0254 | 3.9892 | 87.246 |
| | $Ce_5Co_{19}$ | R-3m (166) | 34.3 | 5.0516 | 48.5590 | 1073.144 |
| | $Pr_5Co_{19}$ | P63 /mmc (194) | 20.1 | 5.0491 | 32.2218 | 711.3913 |

Table 1 lists the phase abundance and lattice parameters of the phases in alloys analyzed by the Rietveld method. It is found that as the rapid solidification rate increases, the total abundance of $A_5B_{19}$ phase in the alloys gradually decreases from 51.1 % (mass fraction, as cast alloy) to 41.3% (15m/s alloy), and then increases to 54.4% (25m/s alloy). This result indicates that higher rapid solidification rate

(>15m/s) can help to form $A_5B_{19}$ phase in the alloy. In addition, the cell volumes of $A_5B_{19}$ phase trends up with increase of the rapid solidification rate. Generally speaking, the increase of cell volume (*V*) of hydrogen-absorbing phase in alloy is beneficial to the maximum discharge capacity of alloy electrodes.

### *3.2 Electrochemical properties*

#### *3.2.1 Characteristics of discharge platform*

Fig. 3 shows the electrochemical plateau curves of $La_4MgNi_{17}Co_2$ alloys during hydrogen desorption. As can be seen from Fig.3, with the increase of rapid solidification rate, two plateaus appear in the discharge curve of 15m/s alloy, and gradually become to one and more flat in that of 25m/s alloy. It is reported [31] that the two plateau regions respectively belong to the $AB_5$-type phase (higher plateau pressure) and $A_5B_{19}$-type phase (lower plateau pressure). Thus it can be recognized that melt spun treatment can obviously affects the plateau of $A_5B_{19}$ phase than that of $AB_5$ phase, and appropriate rapid solidification rate can improve the homogenization of alloy.

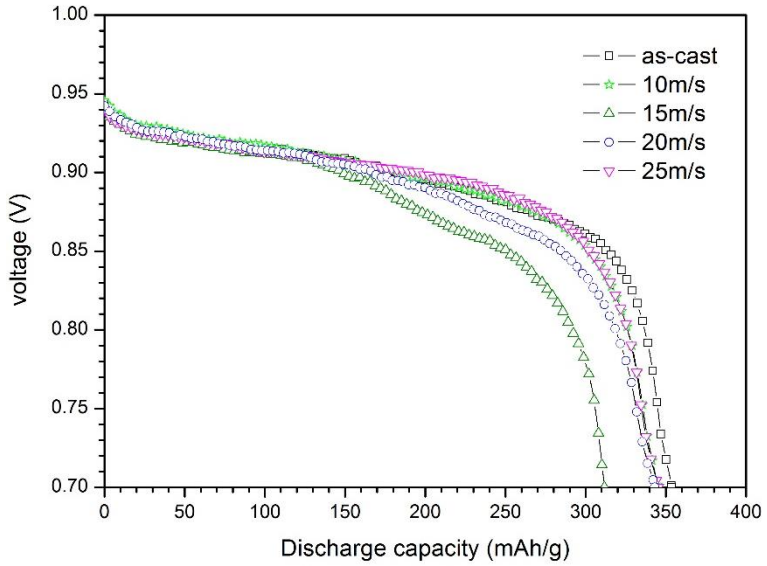


**Figure 3.** Electrochemical plateau curves of $La_4MgNi_{17}Co_2$ alloys during hydrogen desorption at 298K

#### *3.2.2 Activation performance and discharge capacity*

Table 2 presents the electrochemical properties of the alloys. It can be seen that alloy electrodes can be activated in 2 cycles, and with the increase of rapid solidification rate, the maximum discharge capacity ($C_{max}$) gradually decreases from 353.52 mAh/g (as cast alloy) to 311.65 mAh/g (15m/s alloy) and then backs up to 345.25 mAh/g (25m/s alloy). It is well accepted that melt spun treatment generally reduces the maximum discharge capacity of the alloy, and $A_5B_{19}$ phase can absorb more hydrogen than $AB_5$ phase. From the results of XRD analysis above, as is known that the phase abundance of $A_5B_{19}$ phase decreases firstly and then increases with the increase of rapid solidification rate, which is

consistent with the variation of maximum discharge capacity of alloy electrodes, but different with the results reported by Lv et al [24]. This result suggests that the increase of cell volume and the change of $A_5B_{19}$-type phase abundance are the main factors affecting the maximum discharge capacity of the melt spun alloys.

**Table 2.** Electrochemical properties of as cast and melt spun $La_4MgNi_{17}Co_2$ alloy electrodes

| Samples | $C_{max}$ (mAh/g) | $N_a$ | HRD(%) | | | $J_0$ (mA/g) | $S_{100}$ (%) | D ($\times10^{-10}cm^2s^{-1}$) |
|---|---|---|---|---|---|---|---|---|
| | | | $HRD_{300}$ | $HRD_{600}$ | $HRD_{900}$ | | | |
| as cast | 353.52 | 2 | 97.79 | 93.04 | 84.99 | 178.79 | 57.20 | 1.231 |
| 10 m/s | 345.06 | 2 | 97.36 | 89.81 | 82.52 | 138.41 | 57.02 | 1.021 |
| 15 m/s | 311.65 | 2 | 94.36 | 87.00 | 78.87 | 110.63 | 54.55 | 0.751 |
| 20 m/s | 343.03 | 2 | 97.71 | 92.92 | 86.95 | 169.81 | 54.77 | 1.302 |
| 25 m/s | 345.25 | 2 | 95.54 | 89.06 | 83.12 | 151.27 | 71.27 | 1.103 |

*3.2.3 High rate discharge-ability*

From Table 2, it is also found that the $HRD_{300}$ of all the alloys exceed 94% at the discharge current of 300 mA/g, and the HRD decreases obviously with the increasing of discharge current, especially for 15m/s alloy, $HRD_{900}$ is only 78.87%. In general, there are two factors influencing the high rate discharge-ability of MH electrode, i.e., the electrochemical reaction rate on the alloy surface and the diffusion rate of hydrogen in the bulk of the alloy [32]. To investigate the factors of discharge kinetics in alloy electrodes, linear polarization and potential-step experiments were carried out on the alloy electrodes respectively, and the results are presented in Fig.4 and Fig.5. According to the obtained curves, the exchange current density ($J_0$) and hydrogen diffusion coefficient ($D$) were calculated and listed in Table 2.

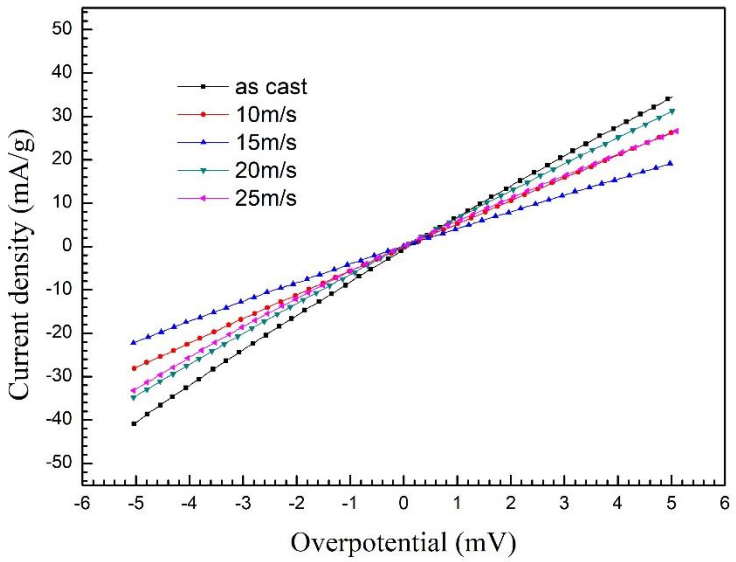


**Figure 4** Linear polarization curves of $La_4MgNi_{17}Co_2$ alloys at 298K

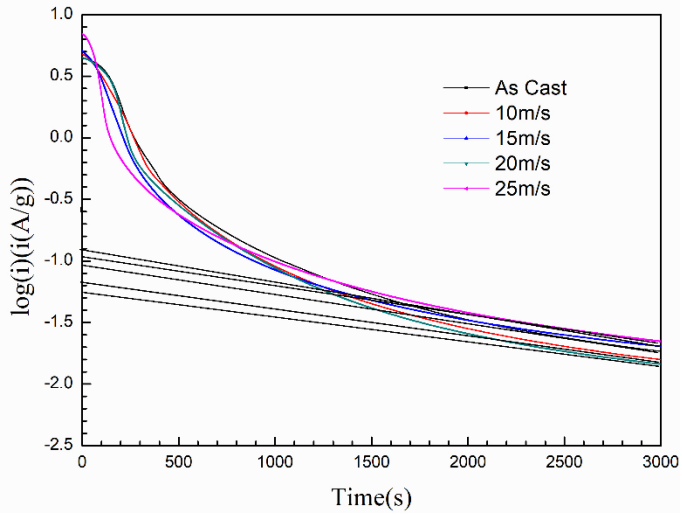


**Figure 5** Semi-logarithmic plots of anodic current-time responses of $La_4MgNi_{17}Co_2$ alloys after +600mV potential-steps at 298K

$J_0$ is calculated by the equation [32]:

$$J_0 = (\frac{RT}{F}) \cdot (\frac{J}{\eta})_{\eta \to 0} \qquad (1)$$

where $J$ is the applied current density (mA/g), $\eta$ is the over-potential (m$V$), and $R$, $F$, $T$ are the gas constant, Faraday constant and absolute temperature respectively.

$D$ is calculated by the equation [33]:

$$\log i = \log(\frac{6FD(C_0 - Cs)}{da^2}) - (\frac{\pi^2}{2.303})(\frac{D}{a^2})\, t \qquad (2)$$

where $D$ is the hydrogen diffusion coefficient ($cm^2/s$), $i$ is the diffusion current density (A/g), $a$ is the radius of spherical alloy particle (cm), $C_0$ and $C_s$ are the initial hydrogen concentration in the alloy or on the electrode surface ($mol/cm^3$), $d$ is the density of the hydrogen storage alloy ($g/cm^3$), $t$ is the discharge time(s) and $F$ is the Faraday constant.

As shown in Table 2, the values of HRD, $J_0$ and $D$ almost have the same variation trend, they gradually decrease to the minimum at 15m/s, and then increase. It is also similar to the phase abundance of $A_5B_{19}$ phase and the cell volume of $LaNi_5$ phase in the XRD analysis mentioned above. It is considered that the inconsistent expansion rate of two phases during absorbing/desorbing hydrogen will cause more internal stress, which increases the degree of pulverization, and thus affects the catalytic reaction area on the surface of the alloys. At the same time, the change of cell volume also affect the diffusion of hydrogen in the alloys. Therefore, the HRD of alloy electrodes are controlled by the electro-catalytic activity on the alloy electrode surface and the hydrogen diffusion coefficient in the alloy bulk.

### *3.2.4 Cyclic stability*

Fig. 6 shows the cyclic stability curves of alloy electrodes. It is observed that melt spun treatment with higher rapid solidification rate can obviously improve the cycle life of alloy electrodes, for example,

the capacity retention rate ($S_{100}$) increases from 57.20% (as cast alloy) to 71.27% (25m/s alloy). In addition, the $S_{100}$ of alloys with lower rapid solidification rate sometimes decrease slightly. It is well known that $A_5B_{19}$ phase can absorb more hydrogen than $AB_5$ phase, and then has larger hydrogen absorption expansion rate. Because of the internal stress between the two phases in the alloy due to the difference of hydrogen absorption expansion rate, the alloy particles are easily pulverized during the charging/discharging process. It is well accepted that a higher degree of pulverization makes the particles expose more surface area to the corrosive electrolyte, then corrode more and have a poor cycling stability. However, with further increase of rapid solidification rate, metallurgical conditions can promote the formation of $A_5B_{19}$ phase, and help to get fine grain and homogeneous composition, which improves the cycle life.

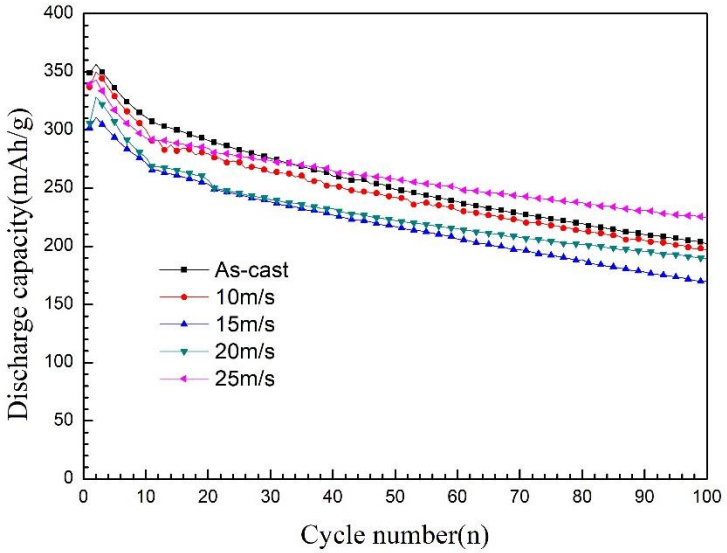


**Figure 6** Cyclic stability curves of $La_4MgNi_{17}Co_2$ alloy electrodes at 298K

## 4. CONCLUSIONS

$La_4MgNi_{17}Co_2$ alloys were prepared by induction melting and melt spun treatment with different rapid solidification rate (10, 15, 20, 25m/s). The XRD analysis revealed that all the alloys are composed of $(La,Mg)_5Ni_{19}$ ($A_5B_{19}$-type) phase and $LaNi_5$ phase, and the Mg element exists in $(La,Mg)_5Ni_{19}$ phase, occupying the same location as in $PuNi_3$ structure. It is found that higher rapid solidification rate (>15m/s) can help to form $A_5B_{19}$ phase. The electrochemical measurements showed that all the alloys have good activation performance (in 2 cycles) and high rate discharge-ability ($HRD_{600}$>87%). Melt spun treatment can obviously affect the plateau of $A_5B_{19}$ phase than that of $AB_5$ phase, and higher rapid solidification rate (25m/s) can improve the maximum discharge capacity ($C_{max}$) and cycling stability. It is found that the changing $C_{max}$ of alloy electrodes with the increasing of rapid solidification rate are related with the phase abundance and cell volumes ($V$) of the two phases, and the improvement of cycling stability is due to the increasing of anti-pulverization of the alloys treated by melt spun method. Compared with the as

cast alloy, the melt spun alloy with 25m/s shows a good comprehensive electrochemical properties ($C_{max}$=345.25 mAh/g, $S_{100}$ = 71.27%, $HRD_{300}$ = 95.54%).

ACKNOWLEDGMENTS
This work was supported by National Natural Science Foundation of China (50901036), Graduate Science and Technology Innovation Project of Jiangsu Province (SJLX_0488), and Priority Academic Program Development of Jiangsu Higher Education Institutions.

**References**

1. Y. Q. Lei, New Energy Materials, Tianjin University Press, (2000) Tianjin, China.
2. Z. Y. Liu, X. L. Yan, N. Wang, Y. J. Chai, and D. L. Hou, *Int. J. Hydrogen Energy*, 36(2011) 4370.
3. T. Kohno, H. Yoshida, F. Kawashima, T. Indaba, I. Sakai, M. Yamamoto, and M. Kanda, *J. Alloys Compd.*, 311(2000) L5.
4. X. Cai, F. S. Wei, X. L. Xu, and Y. Zhang, *J. rare earths*, 34(2016) 1235.
5. F. S. Wei, X. Cai, Y. Zhang, and F. N. Wei, *Int. J. Electrochem. Sci.*, 12(2017) 429.
6. F. S. Wei, L. Li, H. F. Xiang, H. Li and F. N. Wei, *Trans. Nonferrous Met. Soc. China*, 22(2012)1995.
7. B. Liao, Y. Q. Lei, L. X. Chen, G. L. Lu, H. G. Wang and Q. D. Wang, *J. Alloys Compd.*, 415(2006) 239.
8. W. Q. Jiang, Z. Q. Lan, L. Q. Xu, G. X. Li and J. Guo, *Int. J. Hydrogen Energy*, 34(2009) 4827.
9. D. H. Wang, Y. P. Zhong, R. X. Yan, Y. C. Luo, and L. Kang, *Rare Metal Materials and Engineering*, 39(2010) 0027.
10. Y. M. Zhao, S. Zhang, X. Liu, W. F. Wang, L. Zhang, Y. Li, and S. M. Han, *J. Hydrogen Energy*, 43(2018) 17809.
11. H. Z. Chi, C. P. Chen, L. X. Chen and Q. D. Wang, *J. Alloys Compd.*, 360(2003) 312.
12. Y. F. Liu, An Investigation on the Phase structure and Electrochemical Properties of the La-Mg-Ni-Co-based hydrogen storage alloys, Doctoral Dissertation of Zhejiang University, (2005) Zhejiang, China.
13. Y. F. Liu, Y. H. Gao, H. Li, M. X. Gao and H. G. Pan, *J. Alloys Compd.*, 509(2011) 675.
14. Y. F. Liu, H. G. Pan, M. X. Gao, R. Li, X. Z. Sun and Y. Q. Lei, *J. Alloys Compd.*, 388(2005) 109.
15. T. Z. Si, Q. A. Zhang, and N. Liu, *J. Anhui University of technology (nature Science)*, 27(2010) 249. (in Chinese)
16. K. Wang, Y. C. Luo, X. Z. Mei, G. Q. Zhang, and L. Kang, *Chinese J. Rare Metals*, 39(2015) 882. (in Chinese)
17. Z. W. Chen, X. Z. Xiao, L. X. Chen, X. L. Fan, L.X. Liu, S. Q. Li, H. W. Ge, and Q. D. Wang, *J. Alloys Compd.*, 585(2014) 307.
18. L. H. Gao,C. P. Chen, L. X. Chen, Q. D. Wang, C. Y. wang, and Y. An, *J. Alloys Compd.*,424(2006) 338.
19. L.X. Liu, L. X. Chen, X. Z. Xiao, C. C. Xu, J. Sun, S. Q. Li, H. W. Ge, and L. J. Jiang, *J. Alloys Compd.*, 636(2015) 117.
20. A. Q. Deng, J. B. Fan, K. N. Qian, and Y. C. Luo, *Acta Physico-Chimica Sinica*, 27(2011) 103. (in Chinese)
21. Y. H. Zhang, T. Yang, T. T. Zhai, Z. M. Yuan, G. F. Zhang, and S. H. Guo, *Trans. Nonferrous Met. Soc.*, 25(2015) 1968.
22. Y. H. Zhang, T. Yang, Y. Cai, F. Hu, Y. Qi, and D. L. Zhao, *J. Rare Earths*, 34(2016) 1241.
23. Y. H. Zhang, H. W. Shang, Y. Q. Li, Z. M. Yuan, F. Hu, Y. Qi, and D. L. Zhao, *J. Wuhan*

*University of Technology(Materials Science)*, 33(2018) 812.
24. W. Lv and Y. Wu, *Journal of Alloys and Compounds*, 789(2019) 547.
25. Y. Zhang, F. S. Wei, J. N. Xiao, X. Cai, *Acta Metall. Sin. (Engl. Lett.)*, 30(2017) 1033.
26. B. Liao, the Phase Structure and Electrochemical Properties of La-Mg-Ni based $AB_3$-type Hydrogen Storage Electrode Alloys, Doctoral Dissertation of Zhejiang University, (2004) Zhejiang, China.
27. F. Li, K. Young, T. Ouchi, and M. A. Fetcenko, *J. Alloys Compd.*, 471(2008) 371.
28. X. F. Yang, Y. C. Luo, L. Kang, *China Foundry Machinery & Technology*, 04(2009) 5. (in Chinese)
29. Y. M. Zhao, S. M. Han, Y. Li, J. J. Liu, L. Zhang, and S. Q. Yang, *Electrochimica Acta*, 152(2015) 265.
30. Y. P. Fan, L. Zhang, C. J. Xue, G. X. Fan, J. J. Liu, B. Z. Liu, and S. M. Han, *Int. J. Hydrogen Energy*, 44(2019) 7402.
31. J. Gao, X. L. Yan, Z. Y. Zhao, Y. J. Chai and D. L. Hou, *J. Power Sources*, 257 (2012) 209.
32. C. Iwakura, T. Oura, and H. Inouse, *Electrochim. Acta*, 41(1996) 117.
33. G. Zheng, B. N.Dopov, and R. E White, *J. Electrochem. Soc.,* 142(1995)2695.